Journal of Magnetic Resonance 209 (2011) 142–148

Contents lists available at ScienceDirect

Journal of Magnetic Resonance

journal homepage: www.elsevier.com/locate/jmr

# Spin-label oximetry at *Q*- and *W*-band

W.K. Subczynski [a], L. Mainali [a], T.G. Camenisch [a], W. Froncisz [b], J.S. Hyde [a,*]

[a] Department of Biophysics, Medical College of Wisconsin, Milwaukee, WI, USA
[b] Department of Biophysics, Faculty of Biochemistry, Biophysics, and Biotechnology, Jagiellonian University, Krakow, Poland

ARTICLE INFO

*Article history:*
Received 29 September 2010
Revised 22 December 2010
Available online 8 January 2011

*Keywords:*
EPR
*Q*-band
*W*-band
Loop-gap resonator
Spin-label
Membrane
Oxygen transport
Saturation-recovery

ABSTRACT

Spin–lattice relaxation times ($T_1$s) of small water-soluble spin-labels in the aqueous phase as well as lipid-type spin-labels in membranes increase when the microwave frequency increases from 2 to 35 GHz (Hyde, et al., J. Phys. Chem. B 108 (2004) 9524–9529). The $T_1$s measured at *W*-band (94 GHz) for the water-soluble spin-labels CTPO and TEMPONE (Froncisz, et al., J. Magn. Reson. 193 (2008) 297–304) are, however, shorter than when measured at *Q*-band (35 GHz). In this paper, the decreasing trends at *W*-band have been confirmed for commonly used lipid-type spin-labels in model membranes. It is concluded that the longest values of $T_1$ will generally be found at *Q*-band, noting that long values are advantageous for measurement of bimolecular collisions with oxygen. The contribution of dissolved molecular oxygen to the relaxation rate was found to be independent of microwave frequency up to 94 GHz for lipid-type spin-labels in membranes. This contribution is expressed in terms of the oxygen transport parameter $W = T_1^{-1}\ (\mathrm{Air}) - T_1^{-1}\ (\mathrm{N_2})$, which is a function of both concentration and translational diffusion of oxygen in the local environment of a spin-label. The new capabilities in measurement of the oxygen transport parameter using saturation-recovery (SR) EPR at *Q*- and *W*-band have been demonstrated in saturated (DMPC) and unsaturated (POPC) lipid bilayer membranes with the use of stearic acid (*n*-SASL) and phosphatidylcholine (*n*-PC) spin-labels, and compared with results obtained earlier at *X*-band. SR EPR spin-label oximetry at *Q*- and *W*-band has the potential to be a powerful tool for studying samples of small volume, ~30 nL. These benefits, together with other factors such as a higher resonator efficiency parameter and a new technique for canceling free induction decay signals, are discussed.



## 1. Introduction

The first reports that oxygen could affect EPR spectra of organic free radicals in solutions via liquid-phase Heisenberg exchange are dated about 50 years ago [1–3]. Later, Povich pointed out that oxygen-broadening of the EPR spectra of spin-labels could be used to measure dissolved oxygen concentration and diffusion in homogeneous solvents [4,5]. Backer et al. [6] applied spin-label oximetry to biological systems. Shortly after, the water-soluble spin probe 3-carbamoyl-2,2,5,5-tetramethyl-3-pyrroline-1-yloxyl (CTPO), which is widely used for spin-label oximetry, was introduced (see Ref. [7] for additional historical details). The first rigorous spin-label oximetric study was carried out by Windrem and Plachy [8], who reported in 1980 profiles of the oxygen diffusion–concentration product across the lipid bilayer membrane obtained from line-broadening measurements of lipid-soluble spin-labels. These early applications were based on oxygen-induced line-broadening of spin-label EPR spectra.

In the beginning of the 1980s, $T_1$-sensitive spin-label oximetry methods were developed at the National Biomedical EPR Center at the Medical College of Wisconsin for measurement of the product of the oxygen diffusion constant and the oxygen concentration in membranes [9–11]. $T_1$-sensitive methods have significant advantages over $T_2$-sensitive methods because $T_1$ (usually 1–10 μs) is from one to three orders of magnitude longer than $T_2$. Additionally, $T_1$-sensitive methods can be applied to any system that can be spin-probed or spin-labeled, without the need for a narrow EPR line or the presence of a resolved superhyperfine structure. $T_1$-sensitive oximetry methods include saturation-recovery (SR) (the absolute $T_1$ method [11–13]), continuous wave saturation [10,14], passage displays [15], and the multiquantum approach [16,17]. Spin-label oximetry can be used as a quantitative method because every collision of oxygen with a spin-label contributes to a change in the EPR spectrum in both $T_1$- and $T_2$-sensitive methods [10,18–20].

The first oximetry measurements using either $T_1$- or $T_2$-sensitive methods were made at *X*-band. The development of loop-gap resonators (LGRs) [21] permitted oximetry measurements to be made at lower microwave frequencies for both analytical samples and small laboratory animals [22,23]. This direction developed into a significant branch of *in vivo* oximetry and imaging in which

* Corresponding author. Address: Department of Biophysics, Medical College of Wisconsin, 8701 Watertown Plank Road, Milwaukee, WI 53226-0509, USA. Fax: +1 414 456 6512.
*E-mail address:* jshyde@mcw.edu (J.S. Hyde).

1090-7807/$ - see front matter © 2011 Elsevier Inc. All rights reserved.
doi:10.1016/j.jmr.2011.01.003

oxygen concentration and the distribution of oxygen in laboratory animals [24–26] and also in humans [24,27] are measured. These measurements are done at L- and S-band using $T_2$-sensitive methods. This direction of research has also stimulated development of new spin-labels including deuterated CTPO [28] and trityls [29], as well as other microscopic particulate probes, lithium phtalocyanine [30], coal-derived particles (fusinite) [31], and India ink [32].

The development of new LGRs [33,34] has allowed transfer of the $T_1$-sensitive SR oximetry method to higher microwave frequencies, including *Q*- and *W*-band, which permits oximetry measurements to be made for very small water-containing samples (~30 nL). In our previous work [35], we reported oximetric data acquired using SR at frequencies from 2 to 35 GHz. Here we present oximetry measurements at *Q*- and *W*-band and discuss advantages of spin-label oximetry at these frequencies, especially for biological samples that can only be obtained in limited quantity. In two previous papers [35,36], we showed that (1) the $T_1$ of water-soluble spin-labels depends on microwave frequency (being longest at *Q*-band), and that (2) the effect of collisions between oxygen and spin-labels on the measured $T_1$ value is independent of frequency up to 35 GHz. Here we extend SR measurements to *W*-band, showing also that the $T_1$ of lipid-type spin-labels in membranes exhibits a maximum value at *Q*-band.

Additionally, we showed that the measured collision rate between the nitroxide moiety and oxygen is the same from 2 to 94 GHz. Although the sensitivity in terms of number of spins required for good SR signals increases markedly with increase in microwave frequency, the "concentration sensitivity" of SR of spin-labels has been found to be substantially independent of microwave frequency. It follows that the best frequency for spin-label oximetry in terms of sensitivity to bimolecular collisions with molecular oxygen is 35 GHz (*Q*-band). However, *W*-band has its own advantages over other frequencies, which are discussed.

## 2. Materials and methods

### 2.1. Materials

One-palmitoyl-2-(n-doxylstearoyl)phosphatidylcholine spin-labels (*n*-PC, *n* = 5, 12, or 16), tempocholine-1-palmitoyl-2-oleoyl-phosphatidic acid ester (T-PC), dimyristoylphosphatidylcholine (DMPC), and 1-palmitoyl-2-oleoylphosphatidylcholine (POPC) were obtained from Avanti Polar Lipids, Inc. (Alabaster, AL). The n-doxylstearic acid spin-label (*n*-SASL, *n* = 5, 10, or 16) and the cholesterol analog, cholestane spin-label (CSL), were purchased from Molecular Probes (Eugene, OR). Other chemicals, of at least reagent grade, were purchased from Sigma–Aldrich (St. Louis, MO).

### 2.2. Sample preparation

The membranes used in this work were multilamellar dispersions of lipids (liposomes) containing 0.5 mol% of *n*-SASL or CSL (in DMPC) or containing 1 mol% *n*-PC or T-PC (in POPC), and were prepared as described previously [37]. The buffer used for measurements with *n*-SASL was 0.1 M sodium borate at pH 9.5. To ensure that all carboxyl groups of SASL were ionized in DMPC membranes, a rather high pH was chosen [38,39]. For other measurements, 10 mM PIPES (piperazine-N,N′-bis(2-ethanesulfonic acid)) and 150 mM NaCl (pH 7.0) were used. Dense liposome dispersions (the loose pellet after centrifugation) with a final spin-label concentration of 1–3 mM were used. The structures of water-soluble and lipid-type spin-labels used in this work and in our previous *Q*- and *W*-band SR measurements [35,36], together with structures of phospholipids, saturated DMPC, and unsaturated POPC, are shown in Fig. 1a and b.

### 2.3. EPR measurements

For EPR measurements, samples were transferred either to a capillary made from the gas-permeable methylpenetene plastic known as TPX (i.d. 0.6 mm; *X*-band) or to a Teflon tube (i.d. 0.2 mm; *Q*-band). Quartz capillaries (i.d. 0.15 mm) were used at *W*-band. At *X*- and *Q*-band, samples were equilibrated directly in the resonator with nitrogen or a mixture of nitrogen and air adjusted with a flowmeter (Matheson Gas Products, model no. 7631 H-604) [20]. The same gas was used for temperature-control. At *W*-band, samples were equilibrated with either nitrogen or air at room temperature outside the resonator, transferred to a quartz capillary, and positioned in the resonator of the *W*-band spectrometer, which is equipped with a temperature-control system. At *W*-band, we also occasionally used the gas exchange method of removing oxygen, placing the sample into a Teflon sample tube and equilibrating it with the gas directly in the resonator. Results were indistinguishable.

Measurements were made using SR capabilities of *X*-, *Q*-, and *W*-band EPR spectrometers. Spectrometers and LGRs used for *Q*- and *W*-band measurements were described earlier [35,36]. For water-soluble spin-labels, the duration of the microwave pulse was 0.3 μs. For lipid spin-labels in membrane suspensions, the pulse duration was 0.3–1 μs. All recovery times acquired in these measurements were single exponential in character. For membrane spin-labels, motion was sufficiently slow that the nitrogen nuclear relaxation times were shorter than the electron $T_1$ values, resulting in strong coupling of the three hyperfine lines. The statement that nuclear relaxation times are sufficiently short arises from the prediction of Yin et al. [40] that if this were not true, multi-exponential recovery times would be observed, contrary to experiment. Experimental knowledge of nitrogen nuclear relaxation times under the conditions of this experiment does not exist to the best of our knowledge.

For both *Q*- and *W*-band SR, the low-field hyperfine line, which is most intense, was observed (Fig. 2; see also Fig. 4 in Ref. [35] for *Q*-band spectra). At *X*-band, the central line was observed.

### 2.4. Data acquisition and processing

Typically, $10^6$ decays were averaged, half of which were off-line and differenced for baseline correction, with 2048 (*X*- and *Q*-band) and 1024 (*W*-band) data points per decay. Sampling intervals depended on sample, temperature, oxygen tension, and microwave frequency, and were from 1–40 ns. Total accumulation time was about 2–5 min. Recovery curves were fitted by single, double, and triple exponentials, and compared. Results indicated that for all of the recovery curves obtained in this work, no substantial improvement in the fitting was observed when the number of exponentials was above one, establishing that recovery curves can be analyzed as single exponentials. Fits were based on a damped linear least-squares method, which utilizes the Gauss–Newton minimization procedure to which a scalar factor is included. This helps to "damp" the process toward the minimum and assures convergence in the iterative steps. The damped least-squares method has proven successful for fitting exponential decay curves [41] and EPR spectra [42]. Fig. 3 shows typical SR curves for 5-PC in POPC membranes from *Q*- and *W*-band measurements in the presence and absence of oxygen. Fits to single exponentials are excellent. Decay time constants were determined with accuracy better than ±3%.

## 3. Results

### 3.1. $T_1$ measurements of deoxygenated samples

In Fig. 4, results obtained in the present work at *W*-band for lipid-type spin-labels *n*-SASL and CSL in saturated DMPC

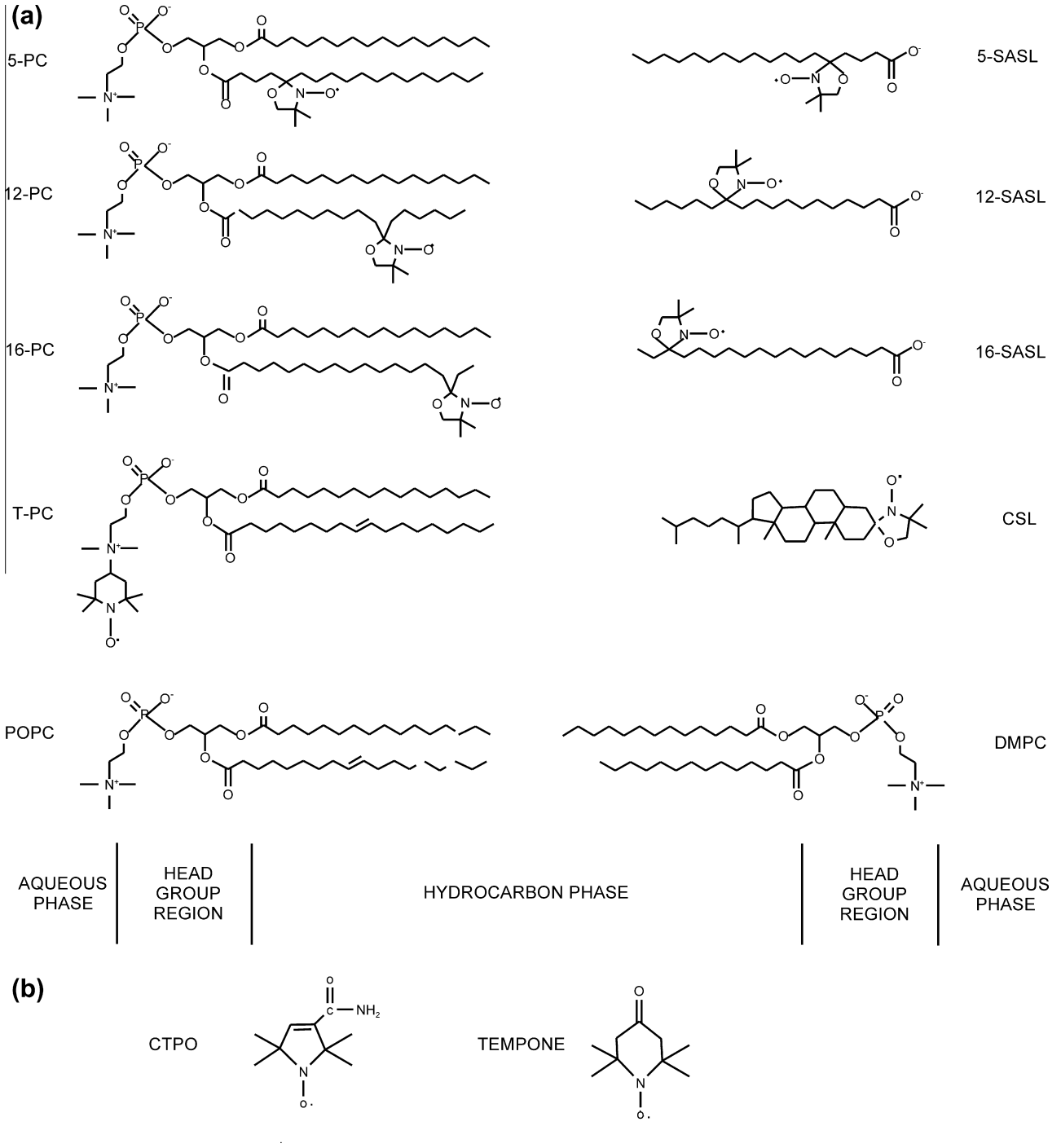


**Fig. 1.** (a) Chemical structures of lipid-type spin-labels together with structures of DMPC and POPC to illustrate approximate locations of nitroxide moieties across the membrane. (b) Chemical structures of water-soluble spin-labels.

membranes (see Fig. 1a for their structures) are combined with previously obtained measurements from the microwave frequency range 2.5–35 GHz [35]. All spin–lattice relaxation times measured at *W*-band are shorter than when measured at *Q*-band. These data confirm again the remarkable fact that the values obtained at 94 GHz depart significantly from the trend observed using data obtained at lower frequencies. Plotted data result in smooth curves, lending credence to the reliability of the surprisingly short times obtained at 94 GHz. It can be concluded that the longest obtainable values for $T_1$ will generally be found at *Q*-band.

Spin-labels CTPO, TEMPONE, and *n*-SASL, together with saturated DMPC membranes, were used in our previous multifrequency measurements for "historical" reasons. Most earlier SR measurements were obtained from these spin-labels in DMPC membranes [11,13,43], which provides reference data. However, the more biologically relevant phospholipid is unsaturated POPC, and the much better lipid-type spin-label analogues are the phospholipid analogues *n*-PC and T-PC, which can be obtained from Avanti Polar Lipids, Inc. (Alabaster, AL). Because of these circumstances, we show in Fig. 5 new data obtained at *X*-, *Q*-, and *W*-band for the phospholipid-type spin-labels (5-, 16-, and T-PC) in unsaturated POPC membranes (see Fig. 1a for these structures). As expected, the longest $T_1$ values were measured at *Q*-band. Values at *X*- and *W*-band were significantly shorter, confirming

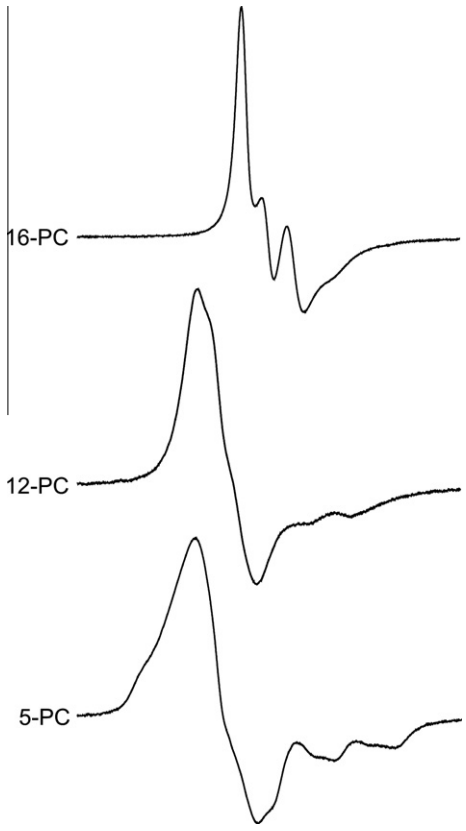


**Fig. 2.** EPR spectra of lipid-type spin-labels in POPC bilayers at *W*-band (25 °C).

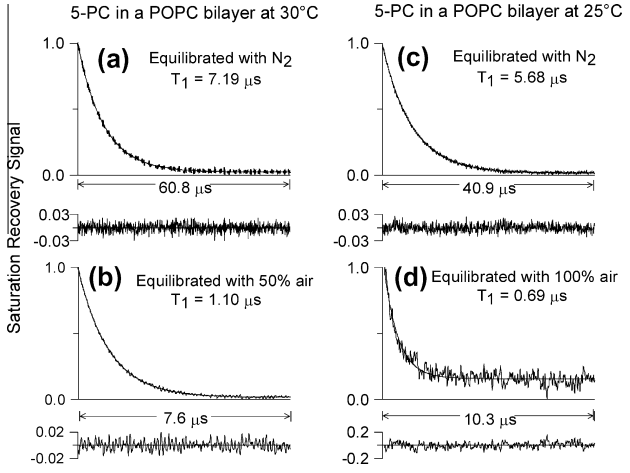


**Fig. 3.** Representative *Q*-band (a, b) and *W*-band (c, d) SR signals with fitted curves and the residuals (the experimental signal minus the fitted curve) of 5-PC in the POPC membrane obtained for samples equilibrated with nitrogen (a, c), 50% air (b, *Q*-band) and 100% air (d, *W*-band). Equilibration with 100% air significantly shortened the $T_1$ value. The available pump power was insufficient to saturate the signal, which lowered the signal-to-noise ratio in (d), nothing that the accumulation time was held constant.

trends observed for other spin-labels in water and membrane environments. The data of Figs. 4 and 5 indicate in all cases that $T_1$ values are shorter at 94 GHz than at 35 GHz. These data indicate that the observed $T_1$ dependence on microwave frequency is independent of the structure of the nitroxide moiety, the structure of the environment of the spin-label, the polarity of the local nitroxide environment (which changes with the depth in the membrane), the rate and anisotropy of motion, and the temperature. This

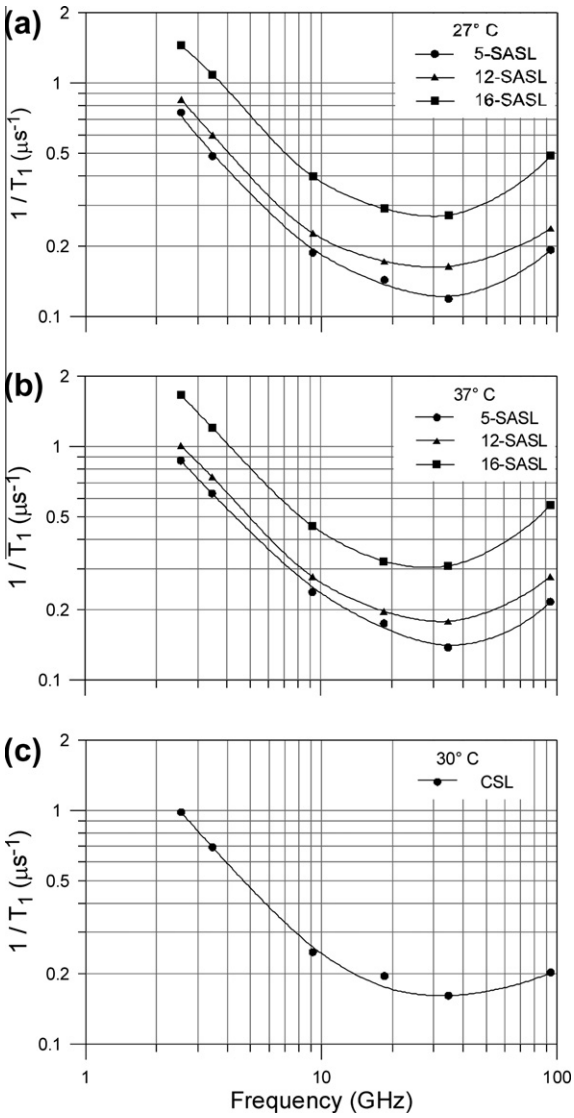


**Fig. 4.** Microwave frequency dependence of the spin–lattice relaxation rate of stearic acid spin-labels (5-, 12-, and 16-SASL) and CSL in saturated DMPC membranes.

experimental finding complements our earlier paper [36], showing data only for CTPO and TEMPONE (see Fig. 1b for these structures). The break in the trend of relaxation rate vs. microwave frequency (Figs. 4 and 5; see also Fig. 8 in Ref. [36]) requires further investigation. Hofbauer et al. [44] report unexpectedly short $T_{1e}$ values for 1 mM solutions of TEMPO in a 10% glycerol–water mixture at *W*-band and suggest a mechanism involving dynamic modulation of the *g*-value.

### 3.2. The oxygen transport parameter

Bimolecular collision rates with oxygen as a function of microwave frequency from 2.54–35 GHz using 16-SASL in DMPC bilayers at 27 °C were reported by Hyde et al. [35]. Data were expressed in terms of the oxygen transport parameter defined by Kusumi et al. [11] by Eq. (1):

$$W(x) = T_1(\mathrm{Air},x) - T_1(\mathrm{N_2},x) \sim D(x)C(x), \quad (1)$$

where $T_1$ values are the spin–lattice relaxation times of the nitroxide in samples equilibrated with atmospheric air and nitrogen, respectively. $W(x)$ is proportional to the product of the local

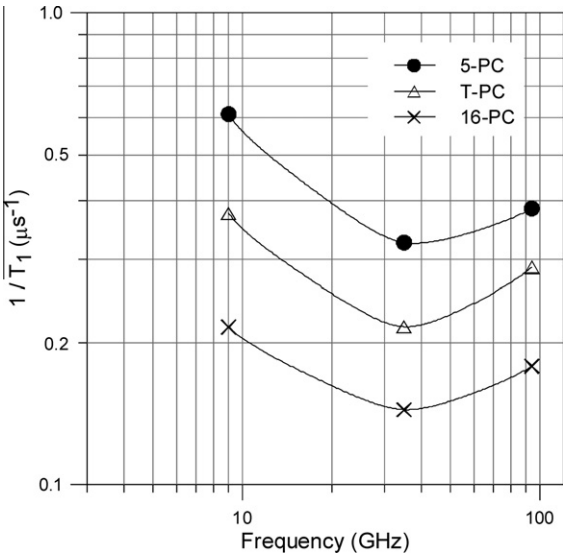


**Fig. 5.** Microwave frequency dependence of the spin–lattice relaxation rate of phospholipid-type spin-labels (5-, 16-, and T-PC) in unsaturated POPC membranes. Measurements at *X*- and *Q*-band were performed at 29–30 °C. Measurements at *W*-band were performed at room temperature.

translational diffusion coefficient $D(x)$ and the local concentration $C(x)$ of oxygen at a "depth" $x$ in the lipid bilayer that is in equilibrium with atmospheric oxygen.

Measurement of the oxygen transport parameter in the same system has been extended to 94 GHz, and all results are presented in Table 1. A new value of 3.02 $\mu s^{-1}$ obtained at 94 GHz is in satisfactory agreement with values reported at lower frequencies. It is concluded that the effect of bimolecular collisions of oxygen on observed spin-label relaxation rates is independent of microwave frequency even at *W*-band, where spin–lattice relaxation times behave anomalously. To emphasize this independence, we added in Table 1 the values of $T_1$s. These values change drastically with microwave frequency, increasing more than five times between 2.54 and 34.6 GHz before decreasing at 94 GHz. These results, together with the fact that the long values of the spin–lattice relaxation times are advantageous for measurement of bimolecular collisions with oxygen, indicate that the best frequency for spin-label oximetry measurements using SR is *Q*-band.

It is notable that for such a large change in microwave frequency (from 2 to 94 GHz), which causes a five-time increase in the spin–lattice relaxation times of lipid-type spin-labels, the oxygen transport parameter measured for the same spin-label at the same temperature is invariant of frequency. Thus, the measured spin–lattice relaxation rate ($T_1^{-1}$) can be related to the oxygen transport parameter, or expressed in frequency-independent oxygen transport parameter units (see Eq. (1)), which we call a frequency-independent ruler or a gold standard for $T_1$ measurements.

### 3.3. Profiles of the oxygen transport parameter across membranes

One of the achievements of spin-label oximetry is the ability to acquire profiles of the oxygen transport parameter across lipid bilayer membranes. These profiles contain significant structural information that is sensed by the solubility and movement of the small hydrophobic molecule, molecular oxygen [11,43,45–47]. They also permit calculation of a significant membrane parameter: namely, the membrane oxygen permeability coefficient, which connects oxygen flux across the membrane with the difference in oxygen concentration in water on both sides of the bilayer [13,48,49]. In Fig. 6, we compared profiles of the oxygen transport parameter across the unsaturated POPC membrane obtained at *X*-, *Q*-, and *W*-band.

Based on the profiles obtained from *X*-, *Q*-, and *W*-band measurements (Fig. 6), values of the oxygen permeability coefficient across the POPC bilayer were evaluated using methods previously described [13]. These values are listed in Table 2. They are independent of microwave frequency within an error of 30% (see Ref. [48] for the minimal and maximal evaluations of the oxygen permeability coefficient across lipid bilayer membranes). These data confirm our conclusion that the results of the oximetry measurements are independent of microwave frequency.

**Table 1**
Spin–lattice relaxation times and oxygen transport parameter vs. microwave frequency obtained from 16-SASL in DMPC bilayers at 27 °C.

| Freq. (GHz) | $S_1$ (2.54) | $S_2$ (3.45) | *X* (9.2) | *K* (18.5) | *Q* (34.6) | *W* (94) |
|---|---|---|---|---|---|---|
| $T_1$ (μs) | 0.69 | 0.94 | 2.54 | 3.46 | 3.69 | 2.05 |
| $W(x)$ ($\mu s^{-1}$) | 2.68 | 2.71 | 2.67 | 2.54 | 2.68 | 3.02 |

## 4. Discussion

The *W*-band capabilities for studying oxygen transport within and across biological membranes at *Q*-band have been discussed previously [35]. In the present paper, we demonstrate measurement of the oxygen transport parameter in model membranes as a function of the depth in the lipid bilayer (Fig. 6). Suspensions of POPC liposomes for *Q*-band measurements were prepared in the same way as for *X*-band measurements. The time of observation at *Q*-band was similar to that at *X*-band (~3 min) as was the signal-to-noise ratio (compare SR signals in Fig. 3a and b with those in Ref. [37]). An LGR, with a sample volume of 30 nL, was used for *Q*-band measurements [35,50], while the sample volume of the LGR used for *X*-band was 3 μL [21]. Feasibility is therefore established for experiments on samples with limited sample volumes. For example, all profiles obtained at *X*-band for calf-[46] and pig-lens [51] lipid membranes were obtained for samples prepared from 50 eyes. Similarly, measurements for cortical and nuclear bovine-lens lipid membranes were based on samples prepared from 100 eyes [47]. Because the sample volume at *Q*-band is 100 times smaller, reliable profiles can, in principle, be obtained based on samples prepared from one eye.

Some recommendations for handling, degassing, and equilibrating with gas-mixture samples of small size are given in Ref. [52]. Yin and Hyde [53] showed that the use of high observing power in SR EPR experiments does not affect the ability to extract bimolecular collision rates and can increase the signal-to-noise ratio up to ten times. Thus, this approach can be used if the signal-to-noise ratio in samples prepared from biological materials is too low. Another way to increase the signal-to-noise ratio is to increase the repetition rate during data acquisition. This approach should be beneficial for measurements at microwave frequencies at which the spin–lattice relaxation time is shorter (for example, at *W*-band compared with *Q*-band).

The results of this paper also demonstrate the ability to make oximetry measurements at *W*-band. Saturation-recovery "concentration sensitivity" has not previously been discussed in the literature. The general conclusion of the present work as well as in previous papers in this series is that SR concentration sensitivity is experimentally found to be independent of microwave frequency. This is one of the significant findings of the present study. However, when sensitivity issues are considered based on the number of spins measured, there is very significant increase in sensitivity as the microwave frequency increases. In the present study, the volume of sample was 30 nL at *Q*- and at *W*-band compared

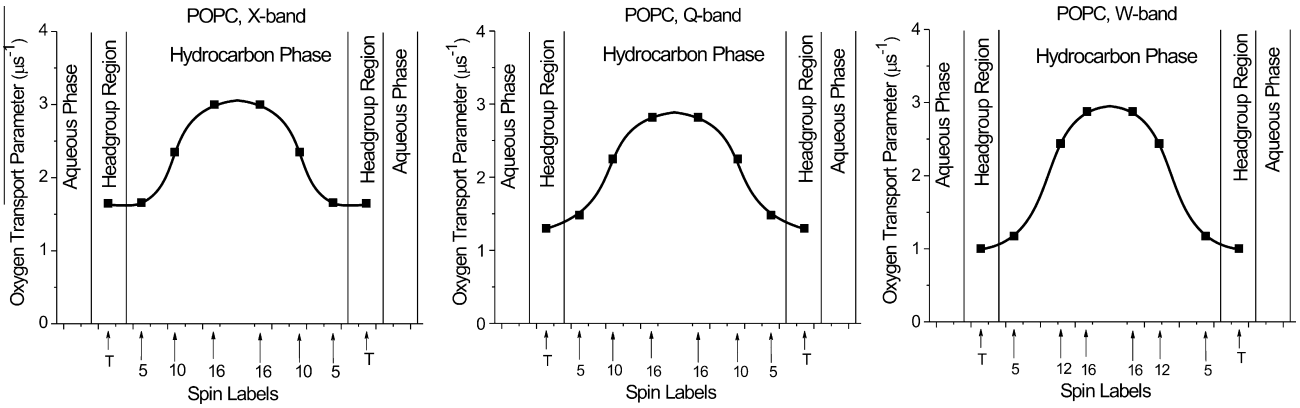


**Fig. 6.** Profile of the oxygen transport parameter across the POPC membrane obtained at *X*-, *Q*-, and *W*-band. Measurements and equilibrations with gas for *X*- and *Q*-band were performed at 29–30 °C. Measurements and equilibrations with gas for *W*-band were performed at room temperature.

**Table 2**
Oxygen permeability coefficient across the POPC bilayer vs. microwave frequency obtained at 29–30 °C (*X*- and *Q*-band) and at room temperature (*W*-band).

| Freq. (GHz) | *X* (9.2) | *Q* (34.6) | *W* (94) |
|---|---|---|---|
| $P_M$ (cm/s) | 112 | 101 | 87 |

with 3 μL at *X*-band, but the SR signal intensity at a fixed accumulation time remained about the same.

A new technique for canceling free induction decay (FID) contamination was introduced for *Q*-band SR [35] and has been extended to *W*-band. In *X*-band, as practiced in this laboratory, the pump and observing power are derived from the same source, and signals are a superposition of FID and SR responses. The technique of 180° pump-phase modulation, which modulates the signal of the FID response but not that of the SR response, permits separation of the superimposed signals. In *Q*- and *W*-band spectrometers, the observing and pump powers are derived from separate synthesizers. The synthesizers are phase-locked, but the pump synthesizer is offset from the observe by a small frequency difference, typically 1 kHz. A benefit of this method is that the two frequencies are well within the spin packet width, but cannot drift with respect to each other. With the pump and observed frequencies separated by this difference, FID signals are effectively averaged away, leaving only the SR signal.

Other significant factors in the experiments presented here are the high resonator efficiency parameter $\Lambda$ (the field produced by 1 W of incident power [54]) and the low resonator quality factor *Q*. The $\Lambda$ is between 10 and 20 for *Q*- and *W*-band LGRs. The LGR with a water sample has a loaded *Q* factor of approximately 100. One significant consequence of high $\Lambda$ and low resonator *Q* is that the dead time between the end of the pulse and the start of data collection can be reduced because there is less stored energy in the resonator when the pulse ends. Shortening of the dead time is crucial for the discrimination by oxygen transport method, which should allow discrimination of domains with high lipid exchange rates [43].

## Acknowledgments

This work was supported by Grants EY015526, EB002052, and EB001980 of the National Institutes of Health.

## References

[1] Y. Deguchi, Proton hyperfine spectra of diphenyl picryl hydrazyl, J. Chem. Phys. 32 (1960) 1584–1585.
[2] K.H. Hausser, Über den einfluß des gelösten sauerstoffs auf die linienbreite der elektron-spin-resonanz in lösung, Naturwissenschaften 47 (1960) 251.
[3] N. Edelstein, A. Kwok, A.H. Maki, Effects of hydrostatic pressure and temperature on spin exchange between free radicals in solution, J. Chem. Phys. 41 (1964) 3473–3478.
[4] M.J. Povich, Measurement of dissolved oxygen concentrations and diffusion coefficients by electron spin resonance, Anal. Chem. 47 (1975) 346–347.
[5] M.J. Povich, Electron spin resonance oxygen broadening, J. Phys. Chem. 79 (1975) 1106–1109.
[6] J.M. Backer, V.G. Budker, S.I. Eremenko, Yu. N. Molin, Determination of the kinetics of biochemical reactions with oxygen using exchange broadening in the ESR spectra of nitroxide radicals, Biochim. Biophys. Acta 460 (1977) 152–156.
[7] W.K. Subczynski, Spin-label oximetry in biological and model systems, Curr. Top. Biophys. 23 (1999) 69–77.
[8] D.A. Windrem, W.Z. Plachy, The diffusion-solubility of oxygen in lipid bilayers, Biochim. Biophys. Acta 600 (1980) 655–665.
[9] C.A. Popp, J.S. Hyde, Effects of oxygen on EPR spectra of nitroxide spin-labels probes of model membranes, J. Magn. Reson. 43 (1981) 249–258.
[10] W.K. Subczynski, J.S. Hyde, The diffusion–concentration product of oxygen in lipid bilayers using the spin-label $T_1$ method, Biochim. Biophys. Acta 643 (1981) 283–291.
[11] A. Kusumi, W.K. Subczynski, J.S. Hyde, Oxygen transport parameter in membranes as deduced by saturation recovery measurements of spin–lattice relaxation times of spin-labels, Proc. Natl. Acad. Sci. USA 79 (1982) 1854–1858.
[12] J.-J. Yin, J.S. Hyde, Spin-label saturation recovery electron spin resonance measurements of oxygen transport in membranes, Z. Phys. Chem. 153 (1987) 57–65.
[13] W.K. Subczynski, J.S. Hyde, A. Kusumi, Oxygen permeability of phosphatidylcholine-cholesterol membranes, Proc. Natl. Acad. Sci. USA 86 (1989) 4474–4478.
[14] C. Altenbach, W. Froncisz, J.S. Hyde, W.L. Hubbell, Conformation of spin-labeled melitin at membrane surface investigated by pulse saturation recovery and continuous wave power saturation electron paramagnetic resonance, Biophys. J. 56 (1989) 1183–1191.
[15] W. Froncisz, C.-S. Lai, J.S. Hyde, Spin-label oximetry: kinetic studies of cell respiration using a rapid-passage $T_1$-sensitive electron spin resonance display, Proc. Natl. Acad. Sci. USA 82 (1985) 411–415.
[16] H.S. Mchaourab, J.S. Hyde, Dependence of the multiquantum EPR signal on the spin lattice relaxation time. Effect of oxygen in spin-label membranes, J. Magn. Reson. B 101 (1993) 178–184.
[17] H.S. Mchaourab, J.S. Hyde, J.B. Feix, Binding and state of aggregation of spin-labeled cecropin AD in phospholipid membranes: effects of surface charge and fatty acyl chain length, Biochemistry 33 (1994) 6691–6699.
[18] J.S. Hyde, W.K. Subczynski, Simulation of ESR spectra of the oxygen-sensitive spin-label probe CTPO, J. Magn. Reson. 56 (1984) 125–130.
[19] W.K. Subczynski, J.S. Hyde, Diffusion of oxygen in water and hydrocarbons using an electron spin resonance spin-label technique, Biophys. J. 45 (1984) 743–748.
[20] J.S. Hyde, W.K. Subczynski, Spin-label oximetry, in: L.J. Berliner, J. Reuben (Eds.), Biological Magnetic Resonance, vol. 8, Spin-labeling: Theory and Applications, Plenum, New York, 1989, pp. 399–425.
[21] W. Froncisz, J.S. Hyde, The loop-gap resonator: a new microwave lumped circuit ESR sample structure, J. Magn. Reson. 47 (1982) 515–521.
[22] S.J. Lukiewicz, S.G. Lukiewicz, *In vivo* ESR spectroscopy of large biological objects, Magn. Reson. Med. 1 (1984) 297–298.
[23] W.K. Subczynski, S. Lukiewicz, J.S. Hyde, Murine *in vivo* L-band ESR spin-label oximetry with loop-gap resonator, Magn. Reson. Med. 3 (1986) 747–754.
[24] W.K. Subczynski, H.M. Swartz, EPR oximetry in biological and model samples, in: S.S. Eaton, G.R. Eaton, L.J. Berliner (Eds.), Biological Magnetic Resonance, Biomedical ESR–Part A: Free Radicals, vol. 23, Metals, Medicine, and Physiology, Kluwer, Boston, 2005, pp. 229–282.

[25] H.J. Halpern, M.K. Bowman, G.R. Eaton, S.S. Eaton, K. Ohno, Low Frequency EPR Spectrometers: MHz Range, EPR Imaging and In Vivo EPR, CRC Press, Boca Raton, FL, 1991. pp. 45–63.
[26] M. Khan, P. Kwiatkowski, B.K. Rivera, P. Kuppusamy, Oxygen and oxygenation in stem-cell therapy for myocardial infarction, Life Sci. 87 (2010) 269–274.
[27] B.B. Williams, N. Khan, B. Zaki, A. Hartford, M.S. Ernstoff, H.M. Swartz, Clinical electron paramagnetic resonance (EPR) oximetry using India ink, Adv. Exp. Med. Biol. 662 (2010) 149–156.
[28] J. Halpern, M. Perik, T.-D. Nguyen, D.P. Spencer, B.A. Teicher, Y.J. Lin, Selective isotopic labeling of a nitroxide spin-label to enhance sensitivity for $T_2$ oximetry, J. Magn. Reson. 90 (1990) 40–51.
[29] J.H. Ardenkjaer-Larsen, I. Laursen, I. Leunbach, G. Ehnholm, L.-G. Wistrand, J.S. Petersson, K. Golman, EPR and DNP properties of certain novel single electron contrast agents intended for oximetric imaging, J. Magn. Reson. 133 (1998) 1–12.
[30] K.J. Liu, M. Moussavi, S.W. Norby, N. Vahidi, T. Walczak, M. Wu, H.M. Swartz, Lithium phthalocyanine: a probe for electron paramagnetic resonance oximetry in viable biological systems, Proc. Natl. Acad. Sci. USA 90 (1993) 5436–5442.
[31] H.M. Swartz, S. Boyer, P. Gest, J.F. Glockner, H. Hu, K.J. Liu, M. Moussavi, S.W. Norby, N. Vahidi, T. Walczak, M. Wu, R.B. Clarjson, Measurements of pertinent concentrations of oxygen in vivo, Magn. Reson. Med. 20 (1991) 333–339.
[32] F. Goda, J.K. Liu, T. Walczak, J.A. O'Hara, J. Jiang, H.M. Swartz, In vivo oximetry using EPR and India ink, Magn. Reson. Med. 33 (1995) 237–245.
[33] W. Froncisz, T. Oles, J.S. Hyde, Q-band loop-gap resonator, Rev. Sci. Instrum. 57 (1986) 1095–1099.
[34] J.W. Sidabras, R.R. Mett, W. Froncisz, T.G. Camenisch, J.R. Anderson, J.S. Hyde, Multipurpose EPR loop-gap resonator and cylindrical TE(011) cavity for aqueous samples at 94 GHz, Rev. Sci. Instrum. 78 (2007) 034701.
[35] J.S. Hyde, J.-J. Yin, W.K. Subczynski, T.G. Camenisch, J.J. Ratke, W. Froncisz, Spin-label EPR $T_1$ values using saturation recovery from 2 to 35 GHz, J. Phys. Chem. B 108 (2004) 9524–9529.
[36] W. Froncisz, T.G. Camenisch, J.J. Ratke, J.R. Anderson, W.K. Subczynski, R.A. Strangeway, J.W. Sidabras, J.S. Hyde, Saturation recovery EPR and ELDOR at *W*-band for spin-labels, J. Magn. Reson. 193 (2008) 297–304.
[37] W.K. Subczynski, R.N.A.H. Lewis, R.N. McElhaney, R.S. Hodges, J.S. Hyde, A. Kusumi, Molecular organization and dynamics of 1-palmitoyl-2-oleoylphosphatidylcholine bilayers containing a transmembrane α-helical peptide, Biochemistry 37 (1998) 3156–3164.
[38] M. Egreet-Charlier, A. Sanson, M. Ptak, O. Bouloussa, Ionization of fatty acids at lipid-water interface, FEBS Lett. 89 (1978) 313–316.
[39] A. Kusumi, W.K. Subczynski, J.S. Hyde, Effects of pH on ESR spectra of stearic acid spin-labels in membranes: probing the membrane surface, Fed. Proc. 41 (1982) 1394.
[40] J.-J. Yin, M. Pasenkiewicz-Gierula, J.S. Hyde, Lateral diffusion of lipids in membranes by pulse saturation recovery electron spin resonance, Proc. Natl. Acad. Sci. USA 84 (1987) 964–968.
[41] S.L. Laiken, M.P. Printz, Kinetic class analysis of hydrogen exchange data, Biochemistry 9 (1970) 1547–1553.
[42] M. Pasenkiewicz-Gierula, W.E. Antholine, W.K. Subczynski, O. Baffa, J.S. Hyde, D.H. Petering, Assessment of the ESR spectra of CuKTSM2, Inorg. Chem. 26 (1987) 3945–3949.
[43] I. Ashikawa, J.-J. Yin, W.K. Subczynski, T. Kouyama, J.S. Hyde, A. Kusumi, Molecular organization and dynamics in bacteriorhodopsin-rich reconstituted membranes: discrimination of lipid environments by the oxygen transport parameter using a pulse ESR spin-labeling technique, Biochemistry 33 (1994) 4947–4952.
[44] W. Hofbauer, K.A. Earle, C.R. Dunnam, J.K. Moscicki, J.H. Freed, High-power 95 GHz pulsed electron paramagnetic resonance spectrometer, Rev. Sci. Instrum. 75 (2004) 1194–1208.
[45] W.K. Subczynski, A. Wisniewska, J.S. Hyde, A. Kusumi, Three-dimensional dynamic structure of the liquid-ordered domain in lipid membranes as examined by pulse-EPR oxygen probing, Biophys. J. 92 (2007) 1573–1584.
[46] J. Widomska, M. Raguz, J. Dillon, E.R. Gaillard, W.K. Subczynski, Physical properties of the lipid bilayer membrane made of calf lens lipids: EPR spin-labeling studies, Biochim. Biophys. Acta 1768 (2007) 1454–1465.
[47] M. Raguz, J. Widomska, J. Dillon, E.R. Gailard, W.K. Subczynski, Physical properties of the lipid bilayer membrane made of cortical and nuclear bovine lens lipids: EPR spin-labeling studies, Biochim. Biophys. Acta 1788 (2009) 2380–2388.
[48] W.K. Subczynski, L.E. Hopwood, J.S. Hyde, Is the mammalian cell plasma membrane a barrier to oxygen transport?, J. Gen. Physiol. 100 (1992) 69–87.
[49] J. Widomska, M. Raguz, W.K. Subczynski, Oxygen permeability of the lipid bilayer membrane made of calf lens lipids, Biochim. Biophys. Acta 1768 (2007) 2635–2645.
[50] C.S. Klug, T.G. Camenisch, W.L. Hubbell, J.S. Hyde, Multiquantum EPR spectroscopy of spin-labeled arrestin K267C at 35 GHz, Biophys. J. 88 (2005) 3641–3647.
[51] M. Raguz, J. Widomska, J. Dillon, E.R. Gailard, W.K. Subczynski, Characterization of lipid domains in reconstituted porcine lens membranes using EPR spin-labeling approaches, Biochim. Biophys. Acta 1778 (2008) 1079–1090.
[52] W.K. Subczynski, C.C. Felix, C.S. Klug, J.S. Hyde, Concentration by centrifugation for gas exchange EPR oximetry measurements with loop-gap resonators, J. Magn. Reson. 176 (2005) 244–248.
[53] J.-J. Yin, J.S. Hyde, Use of high observing power in electron resonance saturation-recovery experiments in spin-labeled membranes, J. Chem. Phys. 91 (1989) 6029–6035.
[54] J.S. Hyde, W. Froncisz, Loop gap resonators, in: A.J. Hoff (Ed.), Advanced EPR: Applications in Biology and Biochemistry, Elsevier, Amsterdam, 1989, pp. 277–306.